

## Supplementary information

### Modelling Electro-Chemically Induced Stresses in All-Solid-State Batteries: Screening Electrolyte and Cathode Materials in Composite Cathodes

Robert Mücke<sup>a</sup>, Najma Yaqoob<sup>a,b</sup>, Martin Finsterbusch<sup>a</sup>, Fadi Al-Jaljoui<sup>a,c</sup>,  
Payam Kaghazchi<sup>a,b</sup>, Dina Fattakhova-Rohlfing<sup>a,d</sup>, Olivier Guillon<sup>a,c</sup>

<sup>a</sup> Forschungszentrum Jülich GmbH, Institute of Energy and Climate Research, Materials  
Synthesis and Processing (IEK-1), 52425 Jülich, Germany;

Jülich Aachen Research Alliance: JARA-Energy, 52425 Jülich, Germany

<sup>b</sup> MESA+ Institute for Nanotechnology, University of Twente, P. O. Box 217, Enschede  
7500AE, The Netherlands

<sup>c</sup> Department of Ceramics and Refractory Materials, Institute of Mineral Engineering, RWTH  
Aachen University, 52064 Aachen, Germany

<sup>d</sup> Faculty of Engineering and Center for Nanointegration Duisburg-Essen, Universität  
Duisburg-Essen, Lotharstr. 1, 47057 Duisburg, Germany.

#### Constitutive equations

A slow uniform decrease in the Li concentration  $x$  leads to a corresponding change in the lattice parameters of the cathode active material resulting in lattice strains (chemical strains)  $\varepsilon_a^{\text{ch}}$ ,  $\varepsilon_b^{\text{ch}}$ ,  $\varepsilon_c^{\text{ch}}$  with  $\varepsilon_b^{\text{ch}} = \varepsilon_a^{\text{ch}}$  as all studied cathode materials were of hexagonal crystallographic structure. The values were just called  $\varepsilon_a$  and  $\varepsilon_b$  in Tab. 1. In tensor notation the lattice strains can be written as (the shear components are 0):

$$\underline{\underline{\varepsilon}}^{\text{ch}} = \begin{pmatrix} \varepsilon_a^{\text{ch}} \\ \varepsilon_a^{\text{ch}} \\ \varepsilon_c^{\text{ch}} \\ 0 \\ 0 \\ 0 \end{pmatrix}$$

For the electrolyte materials there is no Li induced strain, and thus  $\underline{\underline{\varepsilon}}^{\text{ch}} = \underline{\underline{0}}$ . The total strain  $\underline{\underline{\varepsilon}}$  is the sum of the Li induced strain  $\underline{\underline{\varepsilon}}^{\text{ch}}$  and the elastic strain  $\underline{\underline{\varepsilon}}^{\text{e}}$  considering the grain orientation:

$$\underline{\underline{\varepsilon}} = \underline{\underline{R}} \underline{\underline{\varepsilon}}^{\text{ch}} + \underline{\underline{\varepsilon}}^{\text{e}}$$

where  $\underline{\underline{R}}$  is the grain-dependent rotation matrix. The stresses  $\underline{\underline{\sigma}}$  are linked by Hooks law to the elastic strains:

$$\underline{\underline{\sigma}} = \underline{\underline{RCR}}^T \underline{\underline{\varepsilon}}^{\text{e}}$$

where  $\underline{C}$  is the stiffness matrix, which is rotated according to the grain orientation  $\underline{R}$ .  $\underline{C}$  is taken directly from Table 1 or calculated from the Young's modulus and Poisson's ratio for the isotropic materials.

### Further results on NCM955

For the sake of clearness only the configuration of NCM955 with highest stresses was given. The stresses of the other degrees of lithiation are summarised in Fig. S1. All other cathode active materials do not show this behaviour.

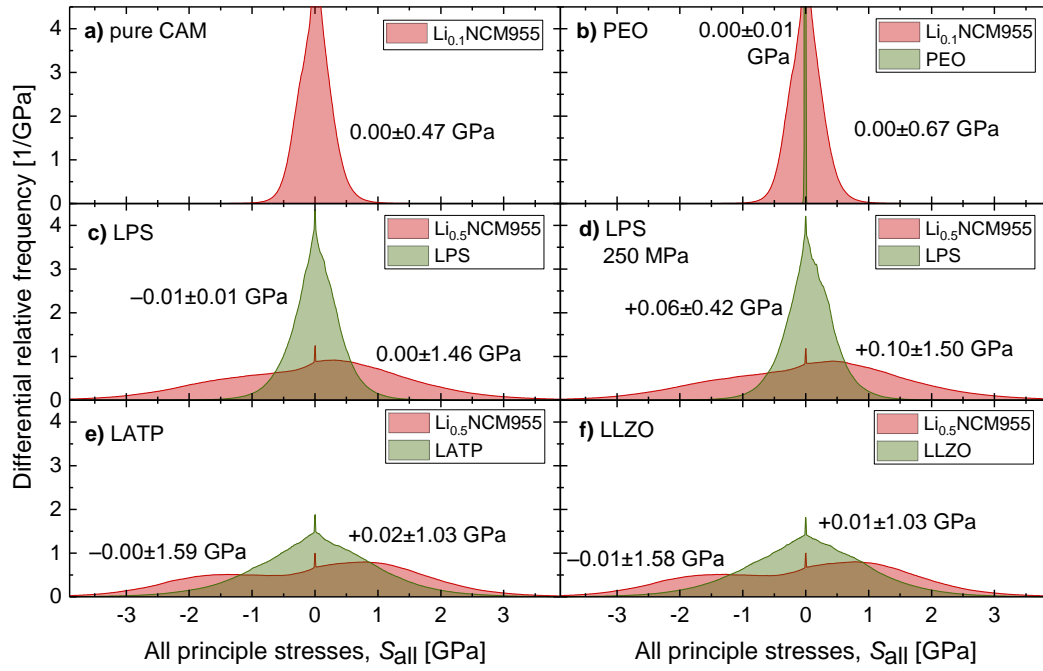


**Fig. S1:** Histograms of all principle stresses of NCM955 at alternative lithiation states for the pure cathode active material and different electrolyte materials in mixed cathodes.

### LPS based cathodes under stack compression

LPS based mixed cathodes are typically compressed up-to 250 MPa in the cell stack. The resulting stresses given in Fig. S2 do not differ significantly from the stresses without cell compression given in the main text (Fig. 2i-l).

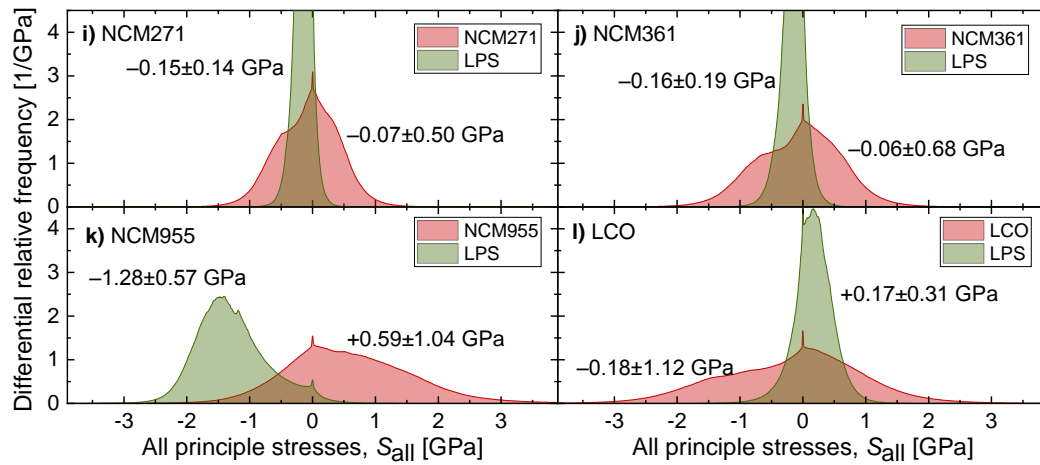


**Fig. S2:** Histograms of all principle stresses of LPS based mixed cathodes with different cathode active materials with a cell pressure of 250 MPa.

### Means stress vs. volume change

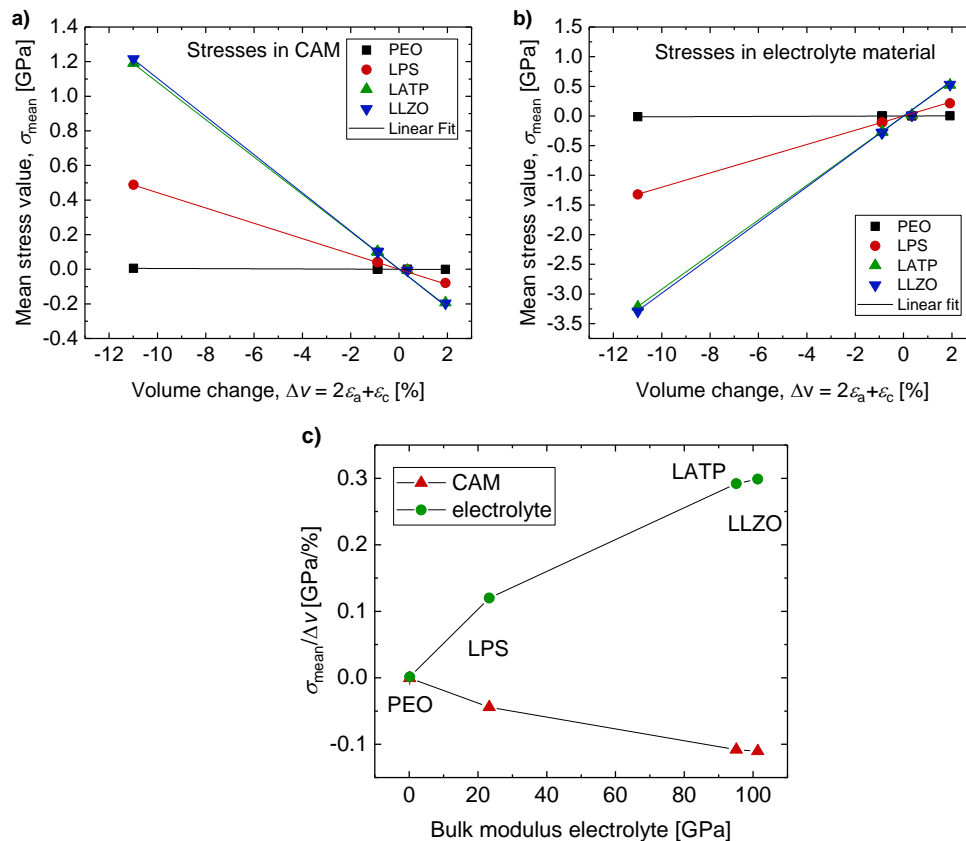


**Fig. S3:** a) Mean stress values  $\sigma_{mean}$  inside cathode active material b) inside electrolyte material as a function of volume change  $\Delta v$  for different electrolyte materials in the composite cathode. c) Corresponding slopes  $\sigma_{mean}/\Delta v$  as a function of bulk modulus of the electrolyte material.

### **Further microstructures**

All material combinations have also been calculated on four different modelled microstructures taken from Ref. 23 with different content of the cathode active material and density (Fig. S4-S7). The results of the dependence of the mean stresses on the electrolyte bulk modulus (sub figures b)-e)) show the same trends as the experimental microstructure in Fig. 3 (also the other results not shown here are comparable). The stress in the CAM and electrolyte materials vs. the free strain mismatch  $\Delta\varepsilon$  were plotted in the sub figures f) and g), respectively. There were used to calculate the proportionality factor in Tab. 1.

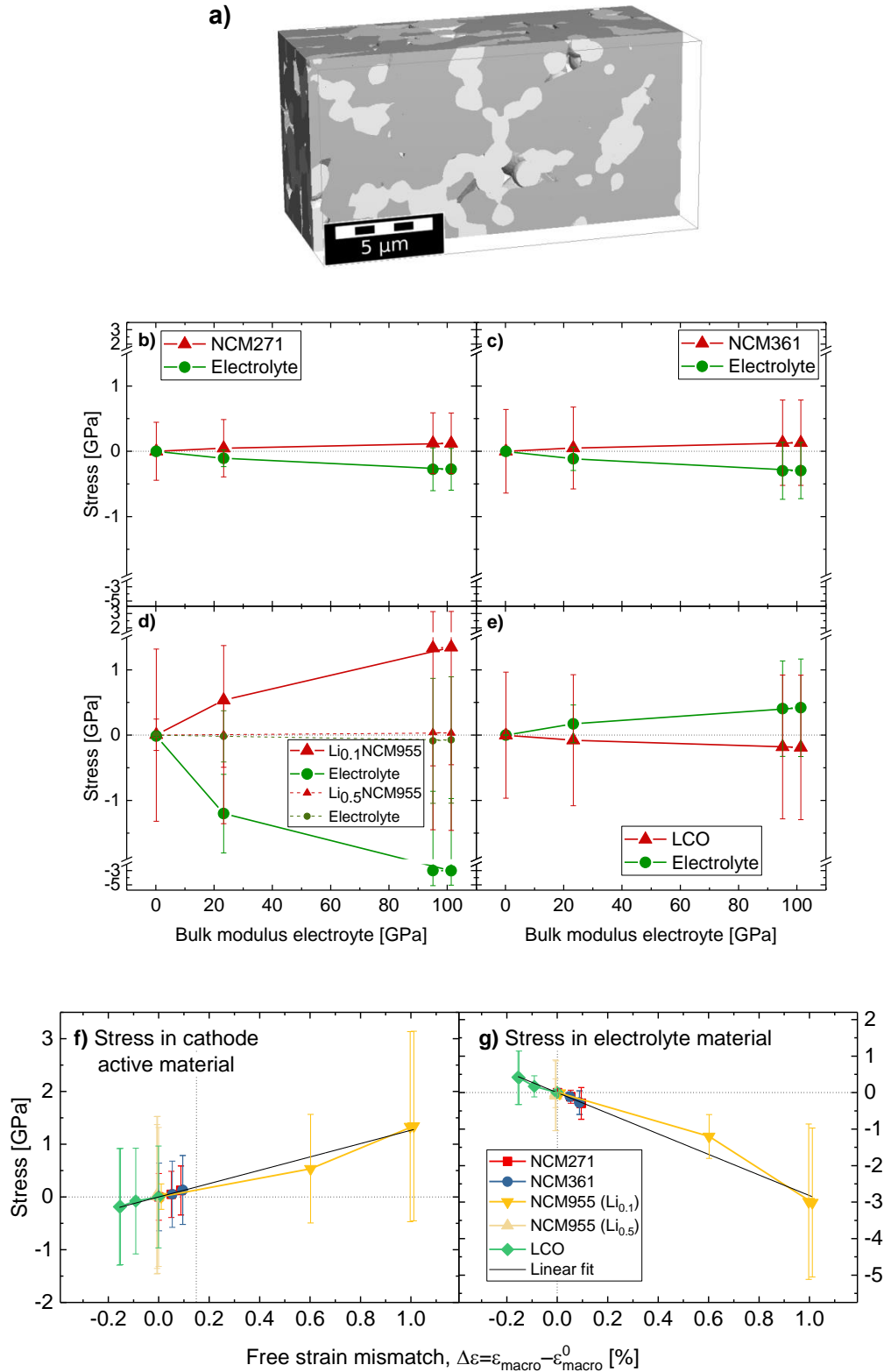


**Fig. S4:** a) Modelled composite cathode microstructure **CAM** (dark) : **Electrolyte** (bright) = **2:1 with a porosity of 7%**. b-e) Average principal stresses inside composite cathodes with different cathode active materials as a function of the bulk modulus of the electrolyte material f) Corresponding stress in CAM g) and electrolyte material of composite cathodes as a function of the free strain mismatch for various cathode active materials. The error bars indicate the width (standard deviation) of the stress distribution.

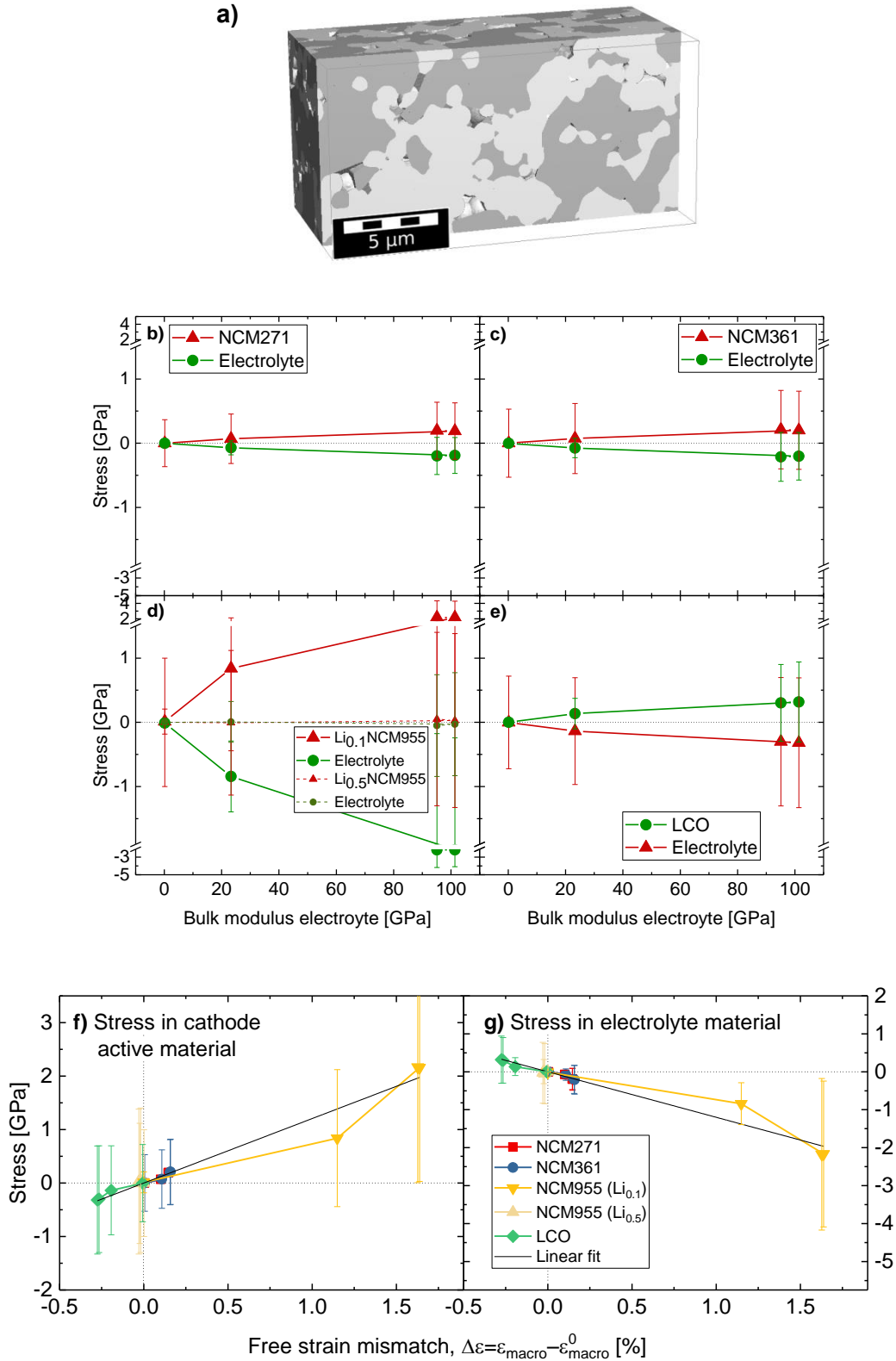


**Fig. S5:** a) Modelled composite cathode microstructure **CAM** (dark) : **Electrolyte** (bright) = **1:1** with a porosity of 7%. b-e) Average principal stresses inside composite cathodes with different cathode active materials as a function of the bulk modulus of the electrolyte material f) Corresponding stress in CAM g) and electrolyte material of composite cathodes as a function of the free strain mismatch for various cathode active materials. The error bars indicate the width (standard deviation) of the stress distribution.

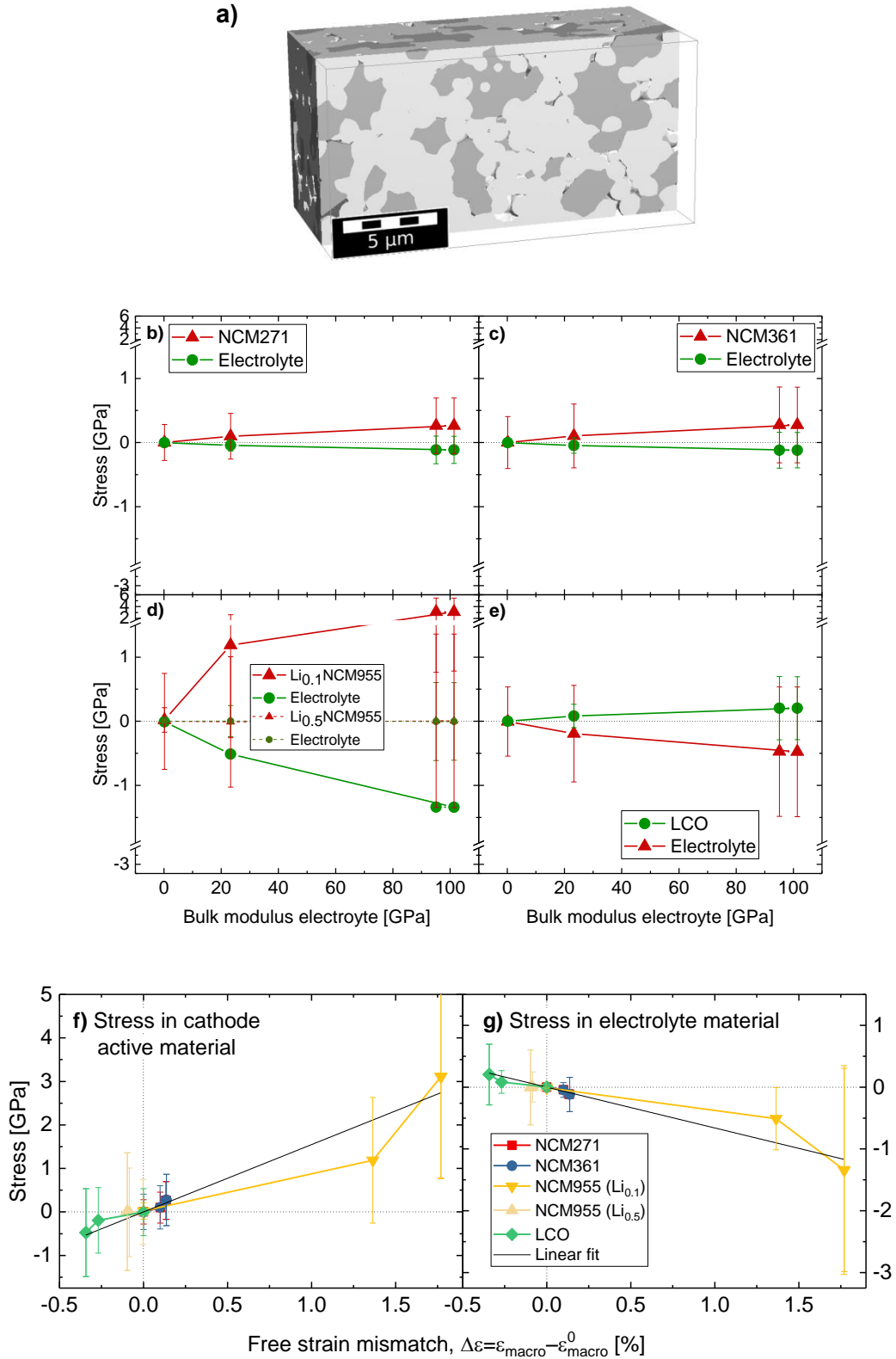


**Fig. S6:** a) Modelled composite cathode microstructure **CAM** (dark) : **Electrolyte** (bright) = **1:2** with a **porosity of 7%**. b-e) Average principal stresses inside composite cathodes with different cathode active materials as a function of the bulk modulus of the electrolyte material f) Corresponding stress in CAM g) and electrolyte material of composite cathodes as a function of the free strain mismatch for various cathode active materials. The error bars indicate the width (standard deviation) of the stress distribution.

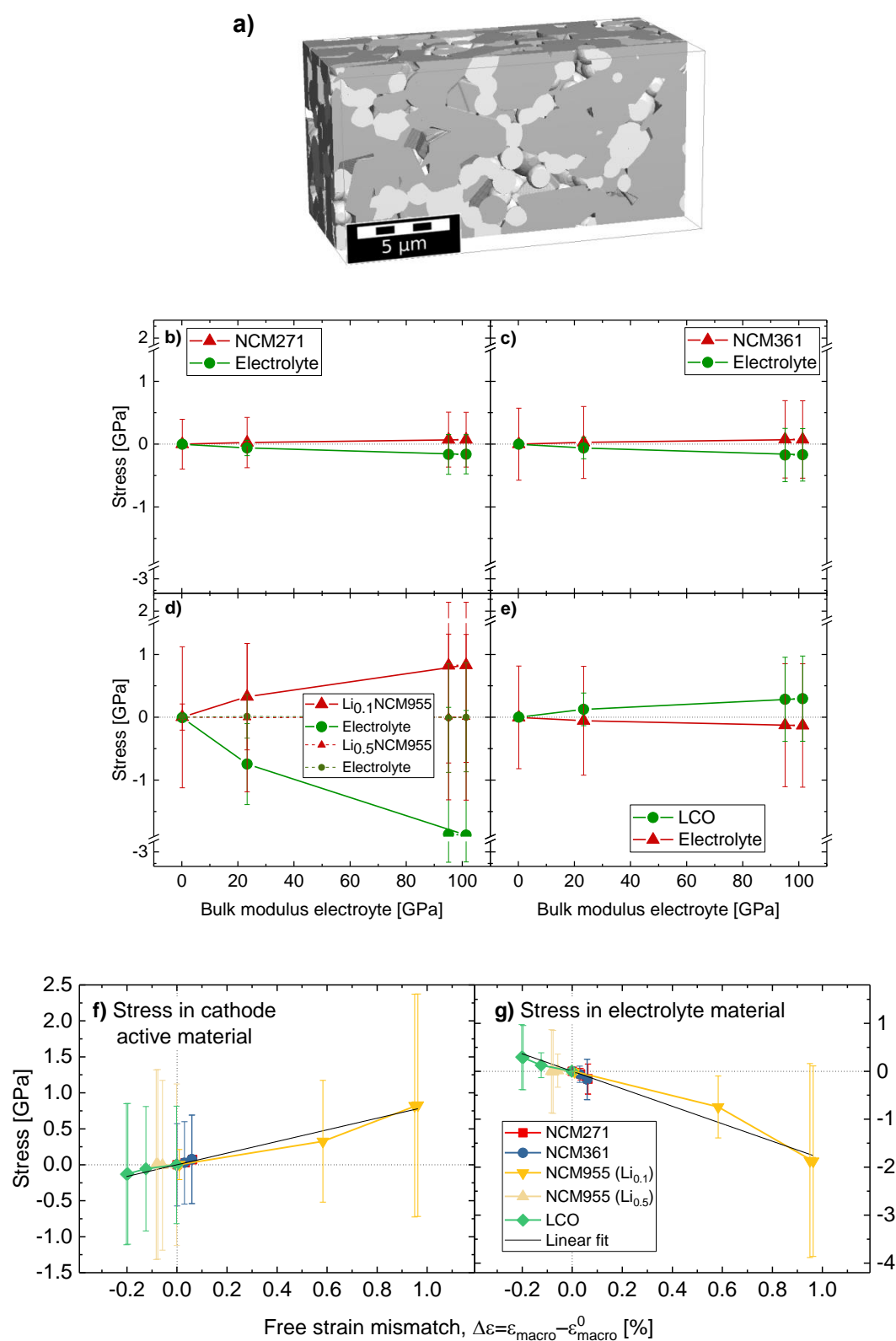


**Fig. S7:** a) Modelled composite cathode microstructure **CAM** (dark) : **Electrolyte** (bright) = **2:1 with a porosity of 20%**. b-e) Average principal stresses inside composite cathodes with different cathode active materials as a function of the bulk modulus of the electrolyte material f) Corresponding stress in CAM g) and electrolyte material of composite cathodes as a function of the free strain mismatch for various cathode active materials. The error bars indicate the width (standard deviation) of the stress distribution.



Tab. S1: Free macroscopic strains of pure randomly oriented cathode active materials  $\varepsilon_{\text{macro}}^0$  for different microstructures compared to the mean lattice strain  $\Delta v/3=(2\varepsilon_a+\varepsilon_c)/3$ . For the modelled structures (Mod.) the volume ratio of CAM:Electrolyte and the porosity in % of the composite cathode are given.

	$\Delta v/3=$ $(2\varepsilon_a+\varepsilon_c)/3$	<b>Exp.</b> <b>structure</b>	<b>Mod.</b> <b>2:1, 7%</b>	<b>Mod.</b> <b>1:1, 7%</b>	<b>Mod.</b> <b>1:2, 7%</b>	<b>Mod.</b> <b>2:1, 20%</b>
<b>Li<sub>0.5</sub>NCM217</b>	-0.29%	-0.29%	-0.31%	-0.30%	-0.23%	-0.29%
<b>Li<sub>0.5</sub>NCM316</b>	-0.30%	-0.31%	-0.32%	-0.32%	-0.24%	-0.29%
<b>Li<sub>0.5</sub>NCM955</b>	0.12%	0.05%	0.01%	0.03%	0.10%	0.09%
<b>Li<sub>0.1</sub>NCM955</b>	-3.66%	-3.67%	-3.67%	-3.62%	-3.01%	-3.66%
<b>Li<sub>0.5</sub>CO<sub>2</sub></b>	0.64%	0.57%	0.56%	0.58%	0.53%	0.61%